Maxim A. Lutoshkin*, Boris N. Kuznetsov and Vladimir A. Levdansky

Spectrophotometric and quantum-chemical study of acid-base and complexing properties of (±)-taxifolin in aqueous solution

https://doi.org/10.1515/hc-2017-0075
Received April 5, 2017; accepted June 29, 2017; previously published online September 15, 2017

Abstract: This study reports the acid-base properties of taxifolin (Tf) in HCl media and aqueous complexation with Ni(II). The equilibrium processes was investigated using a spectrophotometric technique and *ab initio* calculations. Equilibrium constant of protonation was determined using a non-linear Cox-Yates method. Analysis of Ni(II)-Tf complex species under metal dominance conditions was performed in tris-buffer solution. For interpretation and verification of experimental results the Def2-SVP/DFT/PBE0/SMD level was used.

Keywords: DFT; ligand; O-donor; taxifolin.

Introduction

Taxifolin (Tf) is a flavonoid, a member of a large family of heterocyclic compounds that are plant and fungus secondary metabolites. Tf is contained in vascular plants, seeds, fruit, vegetables, red wine and tea [1].

Tf exhibits pronounced inhibitory [2], antioxidant [3, 4], anticarcinogenic [5] and chelating [6] properties. It possesses P vitamin activity [7] and shows antidiabetic [8] and immunoregulatory [9] features, in addition to other properties [10–12]. Some of the metal complexes exhibit antimicrobial, anti-proliferative and other biologically properties [6, 13–16].

***Corresponding author: Maxim A. Lutoshkin,** Université de Lyon, Université Claude Bernard Lyon 1, CNRS, UMR 5256, IRCELYON, Institut de recherches sur la catalyse et l'environnement de Lyon, Villeurbanne, France; and Institute of Chemistry and Chemical Technology SB RAS, Federal Research Center "Krasnoyarsk Science Center SB RAS", Krasnoyarsk 660049, Russian Federation, e-mail: maximsfu@yahoo.com
Boris N. Kuznetsov and Vladimir A. Levdansky: Institute of Chemistry and Chemical Technology SB RAS, Federal Research Center "Krasnoyarsk Science Center SB RAS", Krasnoyarsk, Russian Federation

Metal ions with Tf are new valuable products which can be used in various branches of pharmacology and chemistry. This report deals with an integrated approach (experimental and quantum-chemical simulation) to describe of the acid-base and complexing properties of Tf in aqueous solution.

Results and discussion

Acid-base properties

Neutral form of Tf at pH 1 has one absorption maximum near 285 nm. Spectrum of Tf in strongly acidic solution has a similar profile but it also shows a shoulder in the region of 290–310 nm. A linear relationship between absorbance and concentration for all forms of Tf indicates the absence of the molecular association in solution. Characteristics of the spectral properties of different forms of Tf are given in Table 1. The UV-vis spectra of Tf at different acidities are shown in Figure 1. All raw spectroscopic data are given in the online supplementary material (Tables S1 and S2). The calculations were performed using extinction at high concentration of HCl as extinction of HTf^+. Determination of the number of main-absorbing species are consistent with the presence of two absorption forms, namely Tf and one tautomer of HTf^+. The obtained value of equilibrium constant of protonation is 3.14 ± 0.04 and $1.38 \cdot 10^3 \pm 110$ in logarithmic and absolute units, respectively. The solvation coefficient or m^*-parameter [17] for this process is 3.65 ± 0.08. For comparison, the values of protonation for other flavonoids, such as quercetin and morin are within 9.0–11.0 logarithmic units [18]. The values of solvation coefficient for indoles, amides and tertiary aromatic amines are 1.3, 0.5–0.6 and 1.4, respectively [19].

Thermodynamic properties of the protonation process were theoretically investigated aiming to check convergence with experimental data. The keto-enol equilibriums of HTf^+ was assessed through the calculation of absolute and relative energies of each possible tautomer. HTf^+ has

Table 1 Molar extinction coefficients ($\varepsilon \cdot 10^{-3} \pm 55$) for different forms of Tf.

Form	270 nm	284 nm	308 nm
Neutral	2.630	3.890	1.738
Protonated	2.455	3.631	2.455
Anionic	3.162	4.074	3.548

seven tautomeric structures (Scheme 1). The DFT simulations (Table S3) are consistent with the suggestion that N3 (Figure 2A) tautomer is the most energetically favorable structure for HTf^{+}. All other isomers are more energetic (≥70 kJ · mol^{-1}) than N3.

Quantum chemical calculations of the protonation constant logK_H were carried out based on the cycle shown in Figure 3 [20]. Using of different computational model with explicit solvation or different solvation model such as COSMO or C-PCM lead to unrealistic theoretical results. In this approximation three main parts of the total free energy in solution $\Delta\Delta G^{solv.}$ were evaluated: total Gibbs energy in gas ΔG^{gas} and liquid $\Delta G^{aq.}$ phases and the zero-point energy correction ΔE^{zpe}.

Contribution of these parameters to total free energy of reaction is shown in Table 2. As can be seen, the model provides discrepancies between the theoretical and experimental logK_H values of less than 0.2 logarithmic units.

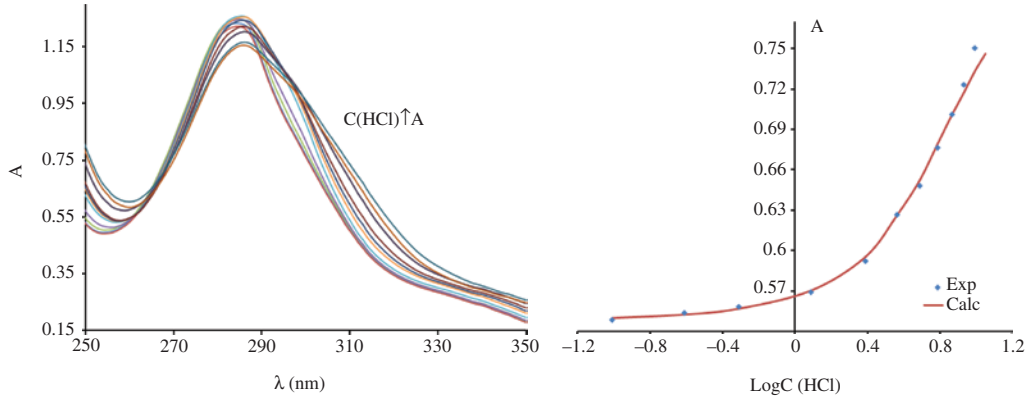

Figure 1 The UV-vis scanning spectra of Tf obtained at various concentration of HCl and absorbance (308 nm) as a function of log([HCl]), [Taxifolin] = 3.16 · 10^{-4} M.

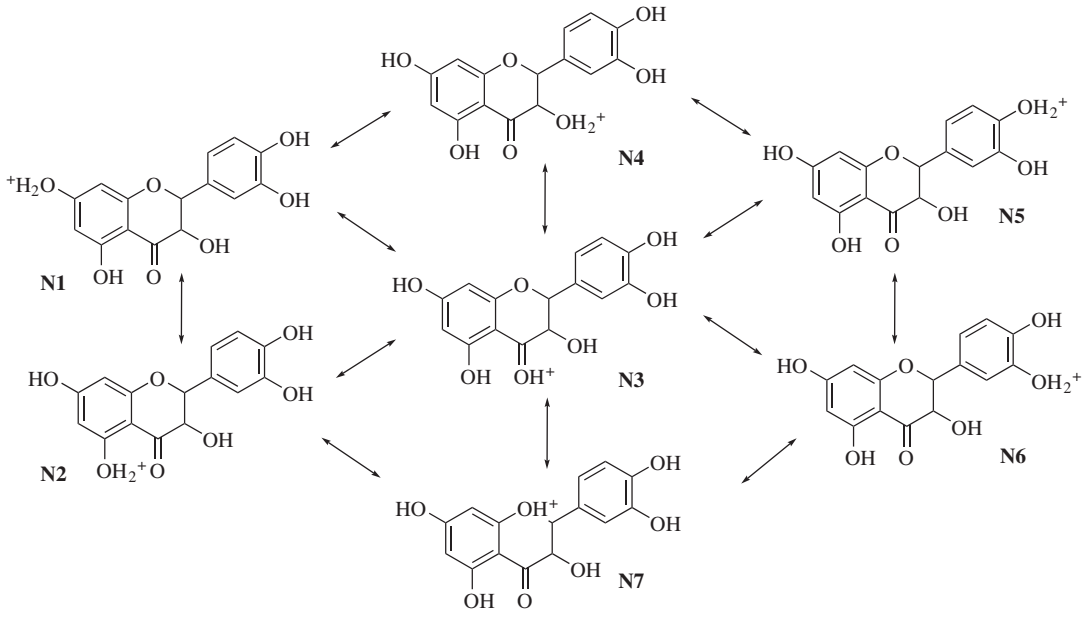

Scheme 1 Keto-enol equilibrium of HTf^{+}.

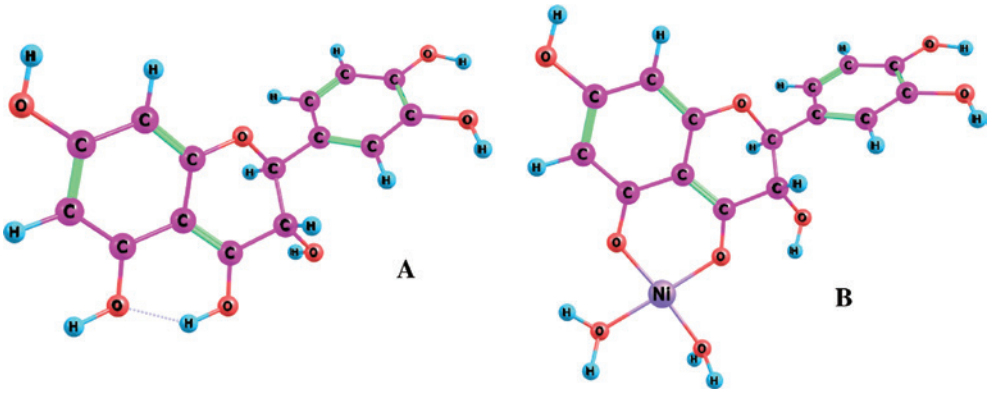

Figure 2 Optimization geometry of HTf^{+} (A) and Ni-Tf (B).

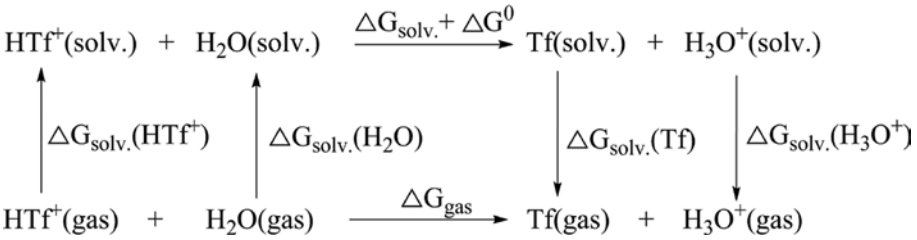

Figure 3 Thermodynamic cycle for quantum-chemical calculation of $\log K_H$.

Table 2 Calculated Gibbs energies and values of zero point energy for $\log K_H$.

Contribution	kJ · mol⁻¹		a.u. · 10⁻³
ΔG^{gas}	23.71		9.03
$\Delta G^{aq.}$	−36.76		−14.25
ΔE^{zpe}	−3.90		−1.48
$\Delta\Delta G^{solv.}$	−16.96		−6.45
$\log K_H^{calc}$		2.97	
$\log K_H^{exp}$		3.14	

Convergence $\log K_H^{calc}$ with $\log K_H^{exp}$ testifies to the correctness of the proposed model of protonation.

Complex formation with Ni(II)

The formation of Ni-Tf complex was indicated by changes in the electronic absorption spectra in solution (Figure 4). The investigation of complexation process in Ni(II)-Tf system was performed under conditions of metal excess. Available pH range for study of this process lie in the range of 7.4–7.8, where Tf exists in mono-anionic form [14]. At pH below 7.4 the interaction Ni^{II}-Tf is too weak to be measured by a spectrophotometric method, and at pH > 7.8 a rapid oxidation of the complex is observed. Interaction between Tf and tris has been not detected under such conditions. Since the ΔA maximum remains invariant at 326 nm (Figure S1) at various nickel concentrations, one might conclude that the complex formation leads to one product (monocomplex species) only with rather negligible contribution from the polynuclear species Ni_nTf_m. Thus, the complexation process of Ni^{2+} with Tf can be described by the equation 1.

$$Ni(H_2O)_4^{2+} + Tf^{-1} \leftrightarrow [Ni(H_2O)_2Tf]^{1-n} + 2H_2O + nH^{+} \quad (1)$$

The value of conditional stability constant ($\log K'$) obtained for this system lies within 2.33–2.38 logarithmic units (Table 3). This value remains unchanged within the specified limits for each acidity. This means that H^{+} does not participate in complexation process and a value of n in equation 1 equals 0. The 'True' $\log K$ cumulative stability constants were obtained from the coefficients of competing reactions [21] (equation 2), in which β_n is the cumulative stability

$$K = \alpha_m K'; \alpha_m = 1 + \sum \beta_n [L^n] \quad (2)$$

constant of competing reactions, K' is conditional stability constant, K is 'true' stability constant. For calculation of the coefficient α_m, the equilibrium constant of Ni(II) hydrolysis

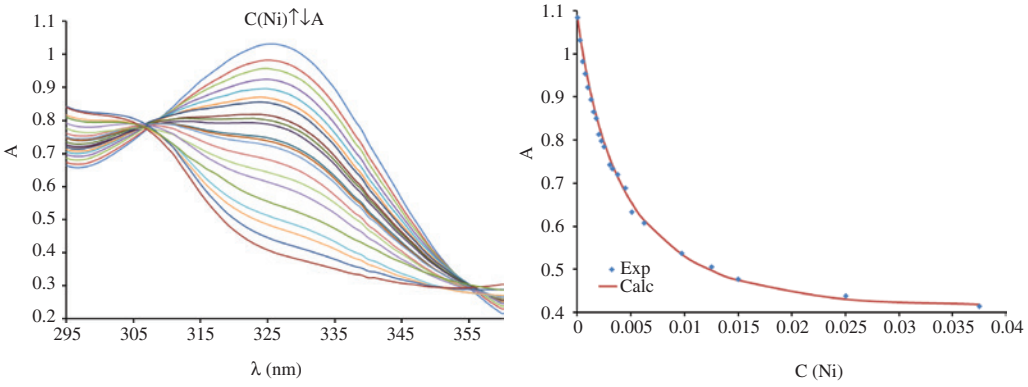

Figure 4 The UV-Vis spectra and absorbance at single wavelength (326 nm) for Ni(II)-Tf system; [Taxifolin] = $2.24 \cdot 10^{-4}$ M; pH = 7.6, I = 1 ($NaClO_4$).

Table 3 Extinction coefficients at 326 nm (ε^{326}), conditional (K') and true (K) stability constants of Ni(II)-Tf complex species in aqueous solution.

pH	logK' ± 0.01	log(ε^{326}) ± 0.02	log$K$ ± 0.08
7.4	2.38	3.13	4.96
7.6	2.36	3.08	5.07
7.8	2.33	3.04	5.17

[22], stability constants of Ni-tris complexes (ML and ML_2 species) [23] and dissociation constant of Tf [14] were used.

The 'true' equilibrium stability constant (log$K$) for Ni-Tf complex is $1.18 \cdot 10^5$ (or 5.1 logarithmic units). This value characterizes the complex as more stable than other complexes of Tf. For example, in the system Cu(II)-Tf the formed monocomplexes have log$K$ values in the range from –15 to –1 logarithmic units [14].

For estimation of keto-enol equilibrium of Ni-Tf complex, the level Def2-SVP/DFT/PBE0/ Stuttgart RSC 1997/SMD was used. According to [6], Tf can exhibit four possible chelating sites with Ni^{II} ion (Scheme 2). The DFT calculations the DFT calculations showed that C1 is the most stable tautomer (Figures S2 and 2B) for the Ni^{II}-Tf structure.

Conclusion

The main parameters of protonation and complexation processes of Tf in aqueous solution were investigated. The obtained value for equilibrium constant of protonation, logK_H, is 3.14 ± 0.04; the stability constant of formation the Ni^{II}-Tf monocomplex, log$K$, is 5.1 ± 0.1. Quantum chemical

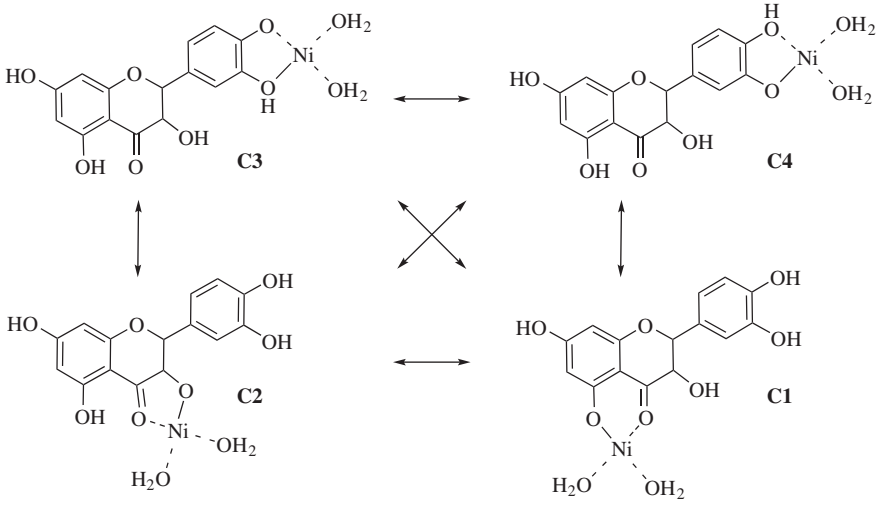

Scheme 2 Keto-enol equilibrium for Ni-Tf complex.

calculations were performed to confirm the proposed coordination models of complexation and protonation.

Experimental

All chemical materials were of analytical grade and used without further purification. The metal salts and ligands were dissolved in distilled water. The concentration of ethanol did not exceed 2% in the final solution. The concentration of HCl was determined by titration with a standardized solution of Na_2CO_3. Buffer solutions within the pH range from 7.00 to 8.00 were prepared with tris and HCl. The concentration of tris in all solutions was 0.05 M. The desired pH values were obtained by adjusting the amount of the buffer components [24]. The ionic strength (I = 1.0) was maintained with $NaClO_4$.

UV-Vis measurements

The Cox-Yates method [25] based on the excess acidity function χ [26] was used to determine the protonation constant (K_H) in strongly acidic solutions (equation 3),

$$A_i = \frac{A_{H_2L} - A_{H_3L^+}}{1 + \left(\frac{C_{H^+}}{K_H}\right) 10^{(m*\chi)}} + A_{H_3L^+} \quad (3)$$

where A_i, A_{H_2L} (ε_{H_2L}), $A_{H_3L^+}$ ($\varepsilon_{H_3L^+}$), and A_{HL^-} (ε_{HL^-}) are the absorbances and molar extinction coefficients of the process solution, the free Tf, and its conjugate acid or base, respectively. The number of absorbing species N contributing to the absorbance matrix was estimated with the factor indication function (IND) [27].

Calculations of conditional stability (K') were performed by nonlinear LSR analysis using the absorbance matrix as raw data [28]. The optimal values for K' and ε^λ were found from the least squares analysis (equations 4 and 5),

$$f(C_{Ni}, C_{Tf}, K', \varepsilon_i) = \sum_{i=1}^{n} (A_i^\lambda - A_{calc}^\lambda)^2 \xrightarrow{K', \varepsilon_i} \min \quad (4)$$

where,

$$A_{calc}^\lambda = \sum_{i}^{n+2} \varepsilon_i [S_i] = \varepsilon_{Tf}[Tf] + \varepsilon_{Ni}[Ni] + \varepsilon_{NiTf}[NiTf] \quad (5)$$

Ab initio study

Ab initio calculations were carried out using the GAMESS US program package [29] with a supercomputer Lomonosov-1 at Moscow State University. The Def2-SVP [30] basis set was applied to H, C and O atoms. Stuttgart RSC 1997 pseudopotentials [31] were applied to Ni(II) for calculation of complexes species. The solvent effects were evaluated using the SMD solvation model [32]. Geometry optimization was performed by density functional theory (DFT). The acid-base equilibrium constants have been calculated using the equations 6–11.

$$pK_H = \Delta\Delta G^{solv.}/(2.303RT) \quad (6)$$

$$\Delta\Delta G^{solv.} = \Delta G^{gas} + \Delta G^{aq.} + \Delta E^{zpe} \quad (7)$$

where

$$\Delta G^{gas} = -G_{gas}(HTf^+) - G_{gas}(H_2O) + G_{gas}(H_3O^+) + G_{gas}(Tf) - \Delta G^0 \quad (8)$$

$$\Delta G^{aq.} = -G_{solv.}(HTf^+) - G_{solv.}(H_2O) + G_{solv.}(H_3O^+) + G_{solv.}(Tf) \quad (9)$$

$$\Delta E^{zpe} = -E_{zpe}(HTf^+) - E_{zpe}(H_2O) + E_{zpe}(H_3O^+) + E_{zpe}(Tf) \quad (10)$$

$$\Delta G^0 = RTln([H_2O]) = 9.964 \text{ kJ/mol}. \quad (11)$$

Here, RTln([H_2O]) is a free energy change associated with moving a solvent from a standard-state solution phase concentration of 1 M to a standard state of the pure liquid, 55.34 M [33, 34]. E^{zpe} is calculated harmonic vibrational frequencies to estimate the zero-point energy correction. Free energies for ionization and solvation processes were used for calculations of ΔG reactions both in the solid state and in solution.

Acknowledgments: The research has been funded by state contract (No 16-43-242083) of Russian Foundation for Basic Research and Government of Krasnoyarsk Region.

References

[1] Kocabova, J.; Fiedlera, J.; Degano, I.; Sokolov, R. Oxidation mechanism of flavanone taxifolin. Electrochemical and spectroelectrochemical investigation. *Electrochim. Acta* **2016**, *187*, 358–363.
[2] Galati, G.; O'Brien, J. Potential toxicity of flavonoids and other dietary phenolics: significance for their chemopreventive and anticancer properties. *Free Radic. Biol. Med.* **2004**, *37*, 287–303.
[3] Kim, Y. J.; Choi, S. E.; Lee, M. W.; Lee, C. S. Taxifolin glycoside inhibits dendritic cell responses stimulated by lipopolysaccharide and lipoteichoic acid. *J. Pharm. Pharmacol.* **2008**, *60*, 1465–1472.
[4] Topal, F.; Nar, M.; Gocer, H.; Kalin, P.; Kocyigit, U. M. Antioxidant activity of taxifolin: an activity-structure relationship. *J. Enzyme Inhib. Med. Chem.* **2016**, *31*, 674–83.
[5] Middleton, E.; Kandaswami, C.; Theoharides, T. C. The effects of plant flavonoids on mammalian cells: Implications for inflammation, heart disease and cancer. *Pharmacol. Rev.* **2000**, *52*, 673–681.
[6] Kasprzak, M. M.; Erxleben, A.; Ochocki, J. Properties and applications of flavonoid metal complexes. *RSC Adv.* **2012**, *5*, 45853–45877.
[7] Afanasev, I. B.; Dorozhko, A. I.; Brodskii, V. V. Kostyuk, A.; Potapovitch, I. Chelating and free radical scavenging mechanisms of inhibitory action of rutin and quercetin in lipid peroxidation. *Biochem. Pharmacol.* **1989**, *38*, 1763–1769.
[8] Haraguchi, H.; Ohmi, I.; Fukuda, A.; Tamura, Y.; Mizutani, K.; Tanaka, O.; Chou. W. H. Inhibition of aldose reductase and sorbitol accumulation by astilbin and taxifolin dihydroflavonols in Engelhardtia chrysolepis. *Biosci. Biotechnol. Biochem.* **1997**, *61*, 651–654.
[9] Schwartz, A.; Middleton, E. Jr. Comparison of the effects of quercetin with those of other flavonoids on the generation and effector function of cytotoxic T lymphocytes. *Immunopharmacol.* **1984**, *7*, 115–126.

[10] Guo, H.; Zhang, X.; Cui, Y,; Zhou, H.; Xu, D.; Shan, T.; Zhang, F.; Guo, Y.; Chen, Y.; Wu, D. Taxifolin protects against cardiac hypertrophy and fibrosis during biomechanical stress of pressure overload. *Toxicol. Appl. Pharmacol.* **2015**, *287*, 168–177.
[11] Sun, X.; Chen, R. C.; Yang, Z. H.; Sun, G. B.; Wang, M.; Ma, X. J.; Yang, L. J.; Sun, X. B. Taxifolin prevents diabetic cardiomyopathy in vivo and in vitro by inhibition of oxidative stress and cell apoptosis. *Food Chem. Toxicol.* **2014**, *63*, 221–232.
[12] Shatalina, Yu. V.; Shubina, V. S. A new material based on collagen and taxifolin: Preparation and properties. *Biophysics* **2015**, *60*, 474–478.
[13] Kostyuk, V. A.; Potapovich, A. I.; Vladykovskaya E. N.; Korkina, L. G. Afanas'ev I.B. Comparative study of antioxidant properties and cytoprotective activity of flavonoids. *Arch. Biochem. Biophys.* **2001**, *385*, 129–137.
[14] Teixeira, S.; Siquet, C.; Alves, C.; Boal, I.; Marques, M. P.; Borges, F.; Lima, J. L.; Reis, S. Structure-property studies on the antioxidant activity of flavonoids present in diet. *Free Radic. Biol. Med.* **2005**, *39*, 1099–108.
[15] Shatalina, Yu. V.; Shubina, V. S. Partitioning of taxifolin–iron ions complexes in octanol–water system. *Biophysics* **2014**, *59*, 351–356.
[16] Lin, L.; Wu, H. Y.; Li, W. S.; Chen, W. L.; Lee, Y. J.; Wu, D. C.; Li, P.; Yeh, A. Kinetic studies of the oxidation of quercetin, rutin and taxifolin in the basic medium by (ethylenediaminetetraacetato) cobalt(III) complex. *Inorg. Chem. Commun.* **2010**, *13*, 633–635.
[17] Hoyuelos, F. J.; Garcia, B.; Ibeas, S.; Munoz, M. S.; Navarro, A. M.; Penacoba, I.; Leal, J. M. Protonation sites of indoles and benzoylindoles. *Eur. J. Org. Chem.* **2005**, *6*, 1161–1171.
[18] Ferrari, V. G.; Pappano, N. B.; Debattista, N. B.; Montan, M. P. Potentiometric and spectrophotometric study of 3-hydroxyflavone-La(III) complexes. *J. Chem. Eng. Data*. **2008**, *53*, 1241–1245.
[19] Petrov, A. I.; Lutoshkin, M. A.; Taydakov, I. V. Aqueous complexation of YIII, LaIII, NdIII, SmIII, EuIII, and YbIII with some heterocyclic substituted β-diketones. *Eur. J. Inorg. Chem.* **2015**, *6*, 1074–1082.
[20] Bryantsev, V. S.; Diallo, M. S.; Goddard, W. A. Calculation of solvation free energies of charged solutes using mixed cluster/continuum models. *J. Phys. Chem. B* **2008**, *112*, 9709–9719.
[21] Burgot, J.-L. Ionic Equilibria in Analytical Chemistry; Springer: Dordrecht, 2012.
[22] Matulis, J.; Slizys, R. On some characteristics of cathodic processes in nickel electrodeposition. *Electrochim. Acta* **1964**, *9*, 1177–1188.
[23] Bologni, L.; Sabatini, A.; Vacca, A. Complex formation equilibria between 2-amino-2(hydroxymethyl)-1,3-propanediol (tris, tham) and Nickel(II), Copper, Zinc(II) and hydrogen ions in aqueous solutions. *Inorg. Chim. Acta* **1983**, *69*, 71–75.
[24] Eliseeva, S. V.; Bünzli, J.-C. G. Rare earths: jewels for functional materials of the future. *New J. Chem.* **2011**, *35*, 1165.
[25] Cox, R. Acidity functions: an update. *Can. J. Chem.* **1983**, *61*, 2225–2229.
[26] Cox, R. The excess acidity of aqueous HCl and HBr media. An improved method for the calculation of X-functions and H. *Can. J. Chem.* **1981**, *59*, 2023–2028.
[27] Meloun, M.; Capek, J.; Miksik P.; Brereton, R. G. Critical comparison of methods predicting the number of components in spectroscopic data. *Analytica Chimica Acta* **2000**, *423*, 51–68.
[28] Grebenyuk, S. A.; Perepichka, I. F.; Popov, A. F. Evaluation of the parameters of 1:1 charge transfer complexes from spectrophotometric data by non-linear numerical method. *Spectrochim. Acta Part A.* **2002**, *58*, 2913–2923.
[29] Schmidt, M. W.; Baldridge, K. K.; Boatz, J. A.; Elbert, S. T.; Gordon, M. S.; Jensen, J. H.; Koseki, S. General atomic and molecular electronic structure system. *Comput. Chem.* **1993**, *14*, 1347– 1363.
[30] Weigend, F.; Ahlrichs, R. Balanced basis sets of split valence, triple zeta valence and quadruple zeta valence quality for H to Rn: Design and assessment of accuracy. *Phys. Chem. Chem. Phys*. **2005**, *7*, 3297–3305.
[31] Bergner, A.; Dolg, M.; Kuechle, W.; Stoll, H.; Preuss, H. Ab initio energy-adjusted pseudopotentials for elements of groups 13–17. *Mol. Phys.* **1993**, *80*, 1431–1441.
[32] Marenich, A. V.; Cramer, C. J.; Truhlar, D. G. Universal salvation model based on solute electron density and on a continuum model of the solvent defined by the bulk dielectric constant and atomic surface tensions. *J. Phys. Chem. B.* **2009**, *113*, 6378–6396.
[33] Vukovic, S.; Hay, B. P.; Bryantsev, V. S. Predicting stability constants for uranyl complexes using density functional theory. *Theor. Inorg. Chem.* **2015**, *54*, 3995–4001.
[34] Kumari, P.; Chandran, P.; Sudheer, K. S. Synthesis and characterization of silver sulfide nanoparticles for photocatalytic and antimicrobial applications. *J. Photochem. Photobiol. B* **2014**, *141*, 235–240.

Supplemental Material: The online version of this article offers supplementary material (https://doi.org/10.1515/hc-2017-0075).